Development of a Fuzzy Logic Based Intelligent System for Autonomous Guidance of Post-stroke Rehabilitation Exercise

Rajibul Huq[1], Rosalie Wang[2], Elaine Lu [1], Debbie Hébert[2,3], Hervé Lacheray [4], and Alex Mihailidis[1,2,3]
[1]Institute of Biomaterials and Biomedical Engineering, University of Toronto, Toronto, Canada
[2] Toronto Rehabilitation Institute, Toronto, Canada
[3]Department of Occupational Science and Occupational Therapy, University of Toronto, Toronto, Canada
[4]Quanser Inc., Markham, ON, Canada
Email addresses: rajibul.huq@utoronto.ca, rosalie.wang@uhn.ca, elaine.lu@utoronto.ca, debbie.hebert@uhn.ca, Herve.Lacheray@Quanser.com and alex.mihailidis@utoronto.ca

***Abstract*—This paper presents preliminary studies in developing a fuzzy logic based intelligent system for autonomous post-stroke upper-limb rehabilitation exercise. The intelligent system autonomously varies control parameters to generate different haptic effects on the robotic device. The robotic device is able to apply both resistive and assistive forces for guiding the patient during the exercise. The fuzzy logic based decision-making system estimates muscle fatigue of the patient using exercise performance and generates a combination of resistive and assistive forces so that the stroke survivor can exercise for longer durations with increasing control. The fuzzy logic based system is initially developed using a study with healthy subjects and preliminary results are also presented to validate the developed system with healthy subjects. The next stage of this work will collect data from stroke survivors for further development of the system.**

Keywords—Upper-limb stroke rehabilitation; robotic reaching exercise; artificial intelligence; haptics; fuzzy logic

I. INTRODUCTION

Stroke is the leading cause of physical disability and death around the world [1, 2]. Research has shown that post-stroke impairments and disabilities can be reduced by intensive, repetitive, and goal-directed rehabilitation [3]. The recovery process, however, is typically slow and labor-intensive, usually involving intensive interaction between a therapist and a patient. One of the main motivations for developing rehabilitation robotic devices is to automate repetitive and physically demanding interventions, which can ease therapists' tasks as well as reduce the health care costs.

The upper extremities are typically affected more than the lower extremities after stroke [4]. There have been several types of robotic devices designed to deliver upper-limb rehabilitation. For example, the work presented in [5] describes basic design considerations and requirements for an upper-limb rehabilitation robot. Researchers have also employed several robot-based therapy techniques for people with paretic upper extremities. The Assisted Rehabilitation and Measurement (ARM) Guide [6] presents "active assist therapy" to help a user to complete a desired reaching task. The Mirror Image Movement Enabler (MIME) therapy system [7] uses a six-degree of freedom (DOF) robot manipulator that applies forces through an orthosis to a user's affected arm in order to accomplish goal-directed movements in 3D space. The GENTLE/s system [8] uses a 3-DOF robot that allows pronation/supination of the elbow as well as flexion and extension of the wrist through a gimbal mechanism. The rehabilitation robotic device that has received the most clinical testing is the MIT-MANUS [9]. It consists of a 2-DOF robot manipulator that assists shoulder and elbow movements by moving the user's hand in the horizontal plane.

Recent work has attempted to make rehabilitation exercises more relevant to daily life activities by mimicking real-life scenarios in virtual reality games [10]. The work presented in [11] integrates virtual reality with adaptive robotic assistance for a 3D haptic system. A similar control approach is used in [12] for self-adaptive robot training, which minimally assists a user to complete a tracking task. Researchers have also started designing adaptive robotic systems using artificial intelligence methods to implement active robotic assistance in rehabilitation tasks. An elbow and shoulder rehabilitation robot [13] was developed using a hybrid position/force fuzzy logic (FL) controller to constrain the movements of the user's arm along a predetermined linear or circular trajectory with a specified load. An artificial neural network (ANN) based adaptive proportional-integral (PI) force controller is presented in [14], where the controller is trained to automatically select appropriate PI gains for each user. There are also available other adaptive control approaches for robot assisted rehabilitation [15], however, most of them are devoted to modeling and prediction of the patients' motion trajectory and assisting them to complete the desired task.

While these robotic systems have shown promising results for upper extremity rehabilitation, most of the systems are unable to adapt the difficulty levels of a rehabilitation exercise; instead the therapists set the difficulty levels during a clinical session.

This work was supported by an NSERC-CIHR Collaborative Research Program grant, Quanser Consulting Inc. and Health Care, Place & Technology (HCTP).

978-1-4673-6024-1/13/$31.00 ©2013 IEEE

The research described in this paper aims to develop an intelligent system that will estimate muscle fatigue [16] of the user during rehabilitation exercise and autonomously adjust task difficulty in terms of resistance or assistance to ameliorate the fatigue. Thus, the system would be able to extend exercise duration to match user performance without any intervention of the therapist. Note that there are many other physiological state variables that might be considered to design the intelligent system. The current system, however, considers only fatigue, which can be estimated using performance variables, e.g. speed, without using biofeedback sensors.

The proposed intelligent system will be implemented with FL [17] to autonomously estimate user fatigue and to generate the desired force control for resistance or assistance. The proposed intelligent system will employ a fuzzy inference system (FIS) [17] for mimicking therapist-like reasoning to autonomously control resistive/assistive forces based on patient fatigue. The proposed system also includes a virtual environment for visual feedback during the exercise. Our previous work [18] also presents an intelligent controller using a partially observable Markov decision process for a reaching rehabilitation task. The work presented in [18], however, uses only discrete resistive forces for autonomous control of the reaching exercise. The work presented in this paper employs continuous values of both resistive and assistive forces in order to improve user performance using the rule-based approach of FL.

The current work only investigates the feasibility of using a fuzzy logic based intelligent controller for automating rehabilitation exercise using estimated muscle fatigue of healthy subjects. However, the contributing muscle fiber distribution ratios for fatigue change with stroke [19, 20]. Neurological changes such as increased tone and other muscle properties that change with stroke, e.g., changed contractile abilities, stiffness and changes in motor units also affect fatigue [20, 21]. The next stage of this work will collect data from stroke survivors to study the effects of these factors for fatigue estimation when using a robotic system.

The rest of the paper describes the robotic system and outlines development of the proposed intelligent system.

II. Rehabilitation System Overview

The current automated upper-limb stroke rehabilitation system consists of two main components: the exercise (Fig. 1) and the robotic system (Fig. 2). Sections II-A and II-B describe the system components.

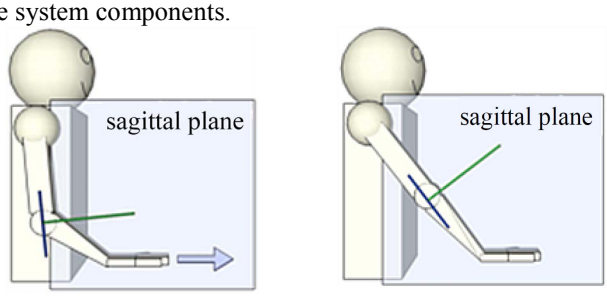

(a) Initial position (b) Final position

Fig. 1. The reaching exercise

A. The exercise

A targeted, load-bearing, forward reaching movement was chosen by consultant stroke therapists as a priority exercise. Reaching is one of the most important abilities to possess, as it is the basic motion involved in many activities of daily living [22]. Fig. 1 provides an overview of the reaching exercise. The reaching exercise is performed in the sagittal plane (aligned with the shoulder) and begins with a slight forward flexion of the shoulder, and extension of the elbow and wrist (Fig. 1(a)). Weight is translated through the heel of the hand as it is pushed forward in the direction indicated by the arrow, until it reaches the target position (Fig. 1(b)). The return path brings the arm back to the initial position. The goal is to have patients gradually reach the furthest target at maximum resistance, while performing the exercise with control (e.g. no deviation from the straight path).

B. Robotic system

Fig. 2 shows the robotic system, which is comprised of the following components: a robotic device, a graphical user interface (GUI) for the therapist, a virtual environment for the patient, and an intelligent system.

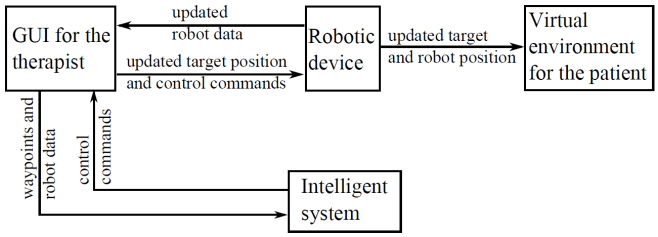

Fig. 2. The reaching rehabilitation system

The non-restraining robotic platform [23], shown in Fig. 3(a), was built by Quanser Inc., a robotics company in Markham, Canada. It has two degrees of freedom, which allows the reaching exercise to be performed in 2D space. The robotic device incorporates haptic technology to provide resistance and assistance during the exercise. Encoders in the end-effector of the robot provide data to indicate hand position during the exercise. Fig. 3(b) shows the virtual environment that provides visual feedback to the patient during the exercise. The robot's end-effector is shown with a hemisphere and the target to be reached with a rectangle. Fig. 3(c) shows the GUI for the therapist. It provides three slider controls to create different haptic effects during the exercise. The first slider is used to create a constant resistive force that repulses the end-effector from the target position. The second slider produces damping effects by creating resistive forces proportional to the speed of the end-effector. The resistive force is directed opposite to the motion direction of the end-effector. The third slider produces a virtual spring effect that creates an assistive force proportional to the distance between the target and the end-effector. The cone-shaped white background represents the workspace of the robot where a therapist can set a target position to be reached by the patient. This panel also shows real-time trajectories of the end-effector during the exercise.

The right panels show instantaneous performance analysis of the reaching exercise.

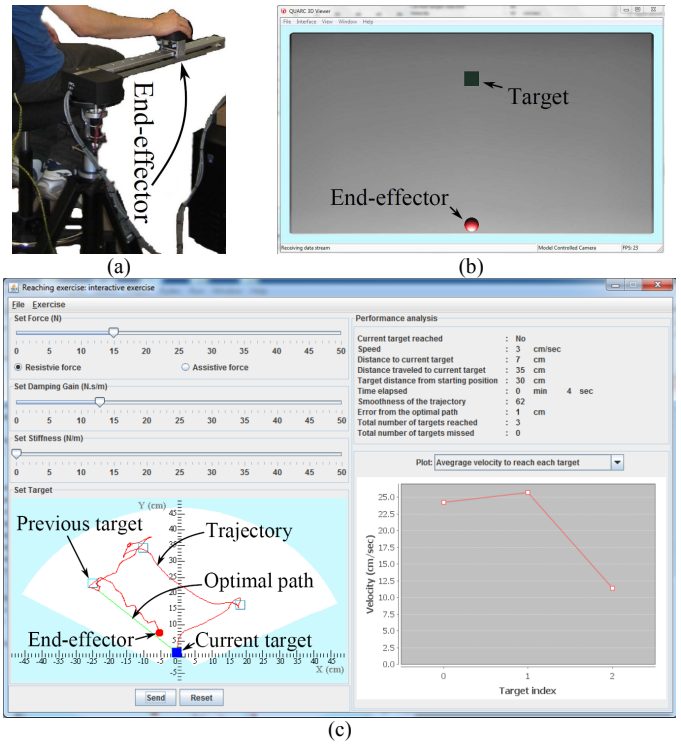

Fig. 3. Components of the robotic system

The GUI provides three modes of operation: 1) interactive, 2) waypoint, and 3) autonomous. This work only presents results for the autonomous mode since the scope of the proposed artificial intelligent system is applicable to only this mode. In the *autonomous* mode, the therapist defines a set of target points and the intelligent system determines the force setting for each target position based on the current performance of the patient. The intelligent system repeats the target positions until the patient becomes fatigued.

The design of the intelligent system consists of two phases – a) study of the effects of different forces on user fatigue during the exercise, and b) design of a system that applies different combinations of forces to recover user fatigue and increase the duration and control performance of the exercise.

C. *Fatigue model*

The design step looks at a very global assessment of fatigue which is closely related to muscle fatigue [16] of fast and slow acting muscle fibers (Type 1 and Type II respectively) [24]. Muscle fatigue is defined as a decreased ability to maintain the expected force or power output and it is commonly experienced after exertion of physical power [25]. The proposed intelligent system assumes that muscle fatigue due to exertion of reaching exercise reduces force outputs of fast and slow twitch fibers resulting in slower speed of the robot end-effector. This work also assumes that control performance (deviation of the end-effector from the optimal path towards the target) of the reaching exercise also deteriorates in the fatigued state of the user.

The following section describes in detail the design steps of the intelligent system and validates the fatigue estimation assumptions.

III. INTELLIGENT SYSTEM

The design step assumes that the constant resistive force towards the target (i.e. a repulsive force from the target) is the most difficult challenge, where a user always needs to control the robot's end-effector to achieve better control performance. The damping force is only activated in the motion state of the end-effector to prevent a user's attempt to reach the target. The spring effect produces assistive forces, which attract the user towards the target.

A. *Effects of different forces on user fatigue*

Considering the types of forces, we set forth the following hypotheses for our study:

Hypothesis 1: Continuously increasing resistive force shortens the exercise duration due to higher user fatigue within a short interval of starting the exercise. In this case, it is assumed that the user will fail to maintain the expected force or power output for longer duration against the continuously increasing resistive forces.

Hypothesis 2: Application of damping force between increasing resistive force extends the exercise duration and results in less user fatigue. In this case, the user has the flexibility to maintain a comfortable speed that balances between speeds and damping forces.

Hypothesis 3: Application of a spring effect together with damping and constant resistive force results in stable control performance in terms of less variation in speed and error, which will produce an ameliorated fatigue state for a longer duration as compared to the previous two cases. In this case, the user can maintain the expected force or power output for longer duration due to the assistive forces.

We conducted three experiments on nine healthy young subjects to validate the hypotheses. The age range of the subjects was 20 - 33 years with an average of 25 years and three of them were female. One of the subjects was a senior high school student and the rest were university students.

Experiment 1 uses a linearly increasing resistive force with an increment of 5N between successive targets. The maximum force applied is 50N. Experiment 2 modifies the previous experiment by inserting a target with a damping force (damping constant, K_d = 25 N.s/m) between successive targets. Experiment 3 inserts one more target with an assistive force (spring constant, K_s = 25 N/m) before the damping force. Table I shows the force patterns specified for the experiments. The target positions were linearly positioned at (0cm, 40cm) and (0cm, 10cm) as shown in Fig. 4. This linear configuration of target positions minimizes the commonly observed speed-accuracy trade off, i.e., higher speeds produces higher errors

and does not significantly affect the control performance of the user in the reaching exercise.

TABLE I
FORCE PATTERNS

Target Index	Experiment 1			Experiment 2			Experiment 3		
	F (N)	K_d $\left(\frac{N.s}{m}\right)$	K_s $\left(\frac{N}{m}\right)$	F (N)	K_d $\left(\frac{N.s}{m}\right)$	K_s $\left(\frac{N}{m}\right)$	F (N)	K_d $\left(\frac{N.s}{m}\right)$	K_s $\left(\frac{N}{m}\right)$
1	0	0	0	0	0	0	0	0	0
2	5	0	0	0	25	0	0	0	25
3	10	0	0	5	0	0	0	25	25
4	15	0	0	5	25	0	5	0	0
5	20	0	0	10	0	0	5	0	25
6	…	…	…	…	…	…	…	…	…

The maximum allowable time to reach each target was set to five seconds. The target positions were repeated until the resistive force reached its maximum level, i.e., F = 50N. The order of experiments was chosen randomly so that the experiments were not biased by continuous improvement in user performance.

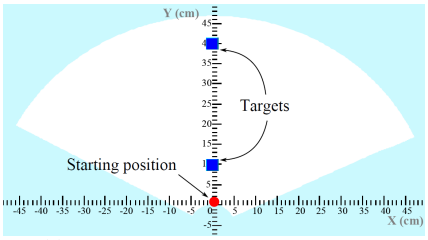

Fig. 4. Target positions

Fig. 5 describes the best-fit (fifth degree polynomial fit) data plots of speed and error with respect to the resultant force applied to the end-effector in the experiments. The experimental results showed that a uniform increase in resistive force resulted in a faster change in fatigue - shown by producing lower speed and higher error values compared to the other two cases (Fig. 5). The participants started the experiments with medium speeds (25~30cm/s) and tried to accelerate in low resistive forces (0~10N).

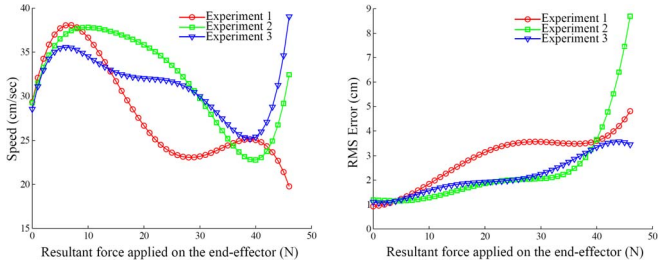

(a) (b)
Fig. 5. Best-fit plots of speed and error of the experiments

Further increase in resistive forces resulted in lower speed values. The results of experiments 2 and 3, however, show an inconsistency where speed increases with high force values (40~50N). This inconsistency was observed because the participants often lost control of the end-effector when the damping and assistive forces were removed while applying very high constant repulsive forces from the target towards the end-effector. This caused high speed movement of the end-effector towards a different direction other than the target. The inconsistency was not observed in experiment 1 where only continuously increasing constant repulsive force was applied and the users adapted to the exercise condition. This phenomenon also indicates that the proposed controller should gradually add or remove the damping and resistive forces while applying high repulsive forces towards the end-effector to avoid unstable situations.

Table II shows the average speed and error along with their standard deviations (SD) obtained in each experiment for all the participants. The average statistics of the experiments shown in Table II support our hypotheses. Experiment 1 has the shortest exercise duration with the lowest speed and highest error.

TABLE II
SUMMARY OF THE EXPERIMENTS (N = 9)

Experiment no.	Speed (cm/s)		Error (cm)		Duration (s)
	Mean	SD	Mean	SD	
1	29.7	18.6	2.5	2.3	24.3
2	33.5	17.0	1.8	1.5	43.8
3	32.0	15.0	1.9	1.4	66.0

This supports Hypothesis 1, where increasing resistive forces fail to maintain higher power outputs (speeds) and lower control errors because of higher fatigue. Hypothesis 2 is also supported by Table II, where average speed and error of experiment 2 are better than those of experiment 1. Hypothesis 3 states that a combination of assistive force with resistive and damping force will result in stable control performance in terms of speed and error variations. It will also produce an improved fatigue state compared to other cases. This case is also evident from Table II where the speed and error variations (standard deviations) and exercise duration of experiment 3 are better than those of the other cases.

Hence, the experimental results support our hypotheses and we propose the following general rules for fatigue estimation and tuning of different forces.

1. Fatigue is high if speed is low and error is high.
2. Fatigue is very high if targets are missed.
3. If fatigue is high then apply assistive force.
4. If fatigue is medium then apply damping and resistive force.
5. If fatigue is low then apply resistive force.
6. If fatigue is very high then stop the exercise.

B. Intelligent system design

The proposed rules in the previous section are the basis of intelligent system design for the reaching exercise. The rules use subjective terms, e.g., low, high and medium, for fatigue estimation and force control. Generally, it is difficult to define hard boundaries for these subjective terms, which may produce frequent switching between different rules and create oscillatory control outputs. A popular solution to this problem is fuzzy logic based decision-making [17], where fuzzy linguistic variables, similar to subjective terms, are used to

form a rule base. The linguistic variables are defined using possibility distribution instead of hard boundaries. As a result, the frequent switching in control output is reduced and smooth transitions between the rules are achieved. Hence, considering the nature of our problem we choose fuzzy logic to design the intelligent system. Fig. 6 shows the decision flow of the proposed intelligent system.

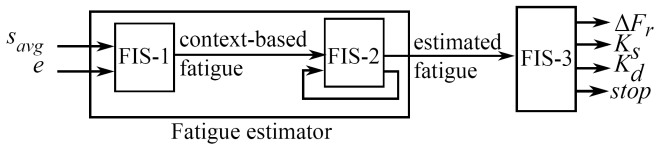

Fig. 6. Intelligent system

Input s_{avg} represents average speed of the end-effector to reach the last target. Input e is defined as follows.

$$e = e_{rms} + \frac{\min\{T_{max}, T_{missed}\}}{T_{max}} \times e_{max} \quad (1)$$

Here, e_{rms} stands for root-mean-squared (RMS) error from the optimal path towards the current target, T_{missed} is the number of successively missed targets in the last T_{max} number of targets, and e_{max} is the allowable maximum range of RMS error. The second part of Eq. (1) adds the effect of missing targets in the error calculation.

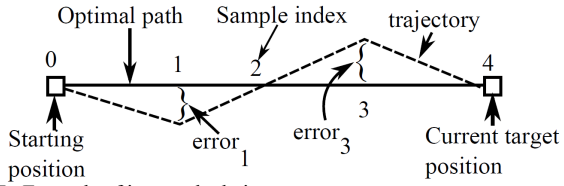

Fig. 7. Example of input calculation

An example of input calculation is described below using Fig. 7, where s_{avg} and e_{rms} are calculated as follows:

$$s_{avg} = \frac{\text{length of trajectory}}{\text{trajectory travel time}} \quad (2)$$

$$e_{rms} = \sqrt{\frac{\sum_i error_i^2}{\text{no. of samples}}} \quad (3)$$

The intelligent system generates four outputs: 1) ΔF_r, change in resistive force, 2) K_d, damping constant, 3) K_s, spring constant, and 4) *Stop* signal to end the exercise. The outputs are further used in Eq. (4)-(6) to generate the resistive, damping, and assistive forces to be applied on the end-effector.

$$F_{r,t} = F_{r,t-1} + \Delta F_r \quad (4)$$

$$F_d = K_d \times s \quad (5)$$

$$F_s = K_s \times l \quad (6)$$

Here, $F_{r,t}$ and $F_{r,t-1}$ denote resistive forces towards the current and previous target positions, s denotes current end-effector speed, and l denotes current distance to the target.

The fuzzy inference system, FIS-1 takes s_{avg} and e as the inputs and calculates user fatigue based on current performance (context-based fatigue). The instantaneous fatigue value may sometimes be erroneous in the case of a corrupted encoder data from the robot. Hence, the fuzzy inference system FIS-2 is used to combine the previously calculated fatigue with the currently measured fatigue. The fuzzy inference system FIS-3 uses the estimated fatigue in order to calculate the output force parameters.

C. Fuzzy inference systems

The FISs used in this work employ Mamdani-Assilian type inference mechanism [20], which uses fuzzy sets for both input and output membership functions (MFs). The input and output linguistic variables of the FISs are defined according to the proposed system shown in Figure 6. The inference mechanism employs min-max-centroid type fuzzy inference system, where the fuzzified input values in a rule are combined using minimum T-norm to establish the rule strength. The output MF corresponding to the rule is then clipped at the rule strength. The aggregation stage uses maximum T-conorm to form an output distribution from the clipped output MFs and finally, the defuzzification stage uses a centroid of area (gravity) method to calculate the final crisp value corresponding to each output variable. This work employs unimodal distributions as MFs for simplicity and a triangular MF is chosen for ease of implementation.

1) FIS-1

Fig. 8 shows the MFs corresponding to the linguistic values of input/output linguistic variables s_{avg}, e, and *fatigue*.

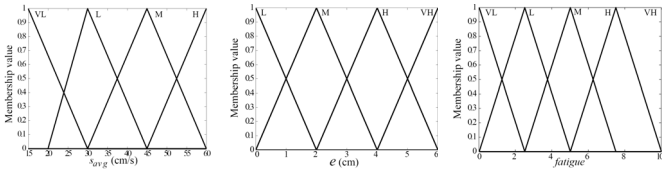

Fig. 8. Input/output membership functions of FIS-1

The linguistic values (fuzzy variables) are defined as follows.

a) Average speed (s_{avg}): The fuzzy variables of s_{avg} are defined using the speed histogram obtained from the experiments in Section III-A. Based on the subjective assessment, the speed range is defined as 15 to 60cm/s, which is further divided into four regions to define four fuzzy variables, namely, *very low* (*VL*), *low* (*L*), *medium* (*M*), and *high* (*H*).

b) Error (e): A similar approach has been followed to define the fuzzy variables associated with e. The error range is defined as 0 to 6cm and four fuzzy variables, namely, *low* (*L*),

medium (*M*), *high* (*H*), and *very high* (*VH*), are uniformly defined over the universe of discourse (see Fig. 8(b)).

c) Context-based fatigue (fatigue): The fuzzy variables associated with this linguistic variable are defined over a universe of discourse with the range of 0 to 10 (see Fig. 8(c)), where 10 indicates the highest fatigue state. We use only five fuzzy variables, namely, *very low* (*VL*), *low* (*L*), *medium* (*M*), *high* (*H*), and *very high* (*VH*), to simplify further rule-base formation in FIS-2. Table III shows the rule-base that relates the input/output fuzzy variables according to the general rules outlined in Section III-A.

TABLE III
RULE-BASE FOR FIS-1

S_{avg}	*E*			
	VH	**H**	**M**	**L**
VL	VH	VH	VH	VH
L	VH	VH	H	M
M	VH	H	M	L
H	VH	M	L	VL

A linear rule formation technique is used for *L*, *M*, and *H* fuzzy variables of the input linguistic variables. More emphasis is given on *VL* and *VH* fuzzy variables to produce very high fatigue. The rule-base is interpreted as follows:

IF s_{avg}=*VL* (*very low*) AND *e*=*VH* (*very high*) THEN *fatigue*=*VH* (*very high*)

2) FIS-2

FIS-2 has two input linguistic variables, *context-based fatigue* and *previous fatigue*, and one output linguistic variable, *estimated fatigue*. The input/output fuzzy variables are described as follows.

a) Context-based fatigue: The output variable of FIS-1 represents this linguistic variable, which uses the same linguistic values as shown in Fig. 8(c).

b) Previous fatigue: This linguistic variable indicates previously estimated user fatigue and uses the same linguistic values as does the context-based fatigue.

c*) Estimated fatigue:* The estimated fatigue also uses five linguistic values to be consistent with the inputs. Table IV shows the rule-base of FIS-2, which relates the input/output fuzzy variables.

TABLE IV
RULE-BASE FOR FIS-2

context-based fatigue	*previous fatigue*				
	VL	**L**	**M**	**H**	**VH**
VL	VL	VL	L	L	M
L	L	L	L	M	M
M	L	M	M	M	H
H	M	M	H	H	H
VH	M	H	H	VH	VH

3) FIS-3

FIS-3 has only one input linguistic variable, *fatigue* and four output linguistic variable, ΔF_r, K_d, K_s, and *stop*. Fig. 10 shows the MFs corresponding to the linguistic values of input/output linguistic variables. The input/output fuzzy variables are described as follows.

a) fatigue: The output variable of FIS-2 represents this linguistic variable, which uses the same linguistic values as shown in Fig. 8(c).

b) Change in resistive force (ΔF_r): Table V shows the rule-base of FIS-3 that relates the input/output fuzzy variables using the general rules outlined in Section III-A. The resistive force F_r is used (by increasing ΔF_r) when *fatigue* is *VL*, *L*, and *M*.

TABLE V
RULE-BASE FOR FIS-3

	Fatigue				
	VL	**L**	**M**	**H**	**VH**
ΔF_r	HP	LP	Z	LN	LN
K_d	L	H	M	L	L
K_s	L	L	M	H	L
stop	NO	NO	NO	NO	YES

The force is reduced to zero (by using negative ΔF_r) when *fatigue* is *H* and *VH*. As a result, we have defined four fuzzy variables, *low negative* (*LN*), *zero* (*Z*), *low positive* (*LP*), and *high positive* (*HP*) for ΔF_r (see Fig. 9(a)).

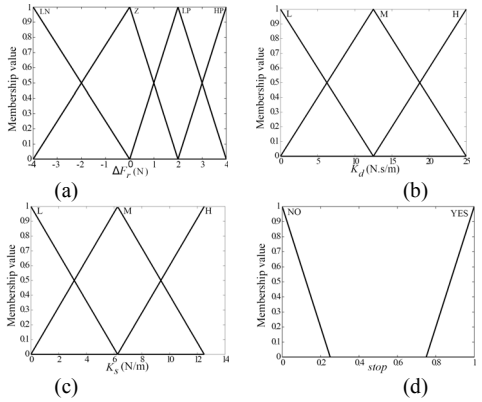

Fig. 9. Output membership functions of FIS-3

c) Damping constant (K_d): The damping force is used when *fatigue* is *L* and *M*, and is reduced to zero otherwise (see Table V). Hence, we have defined three fuzzy variables, *low* (*L*), *medium* (*M*), and *high* (*H*) as shown in Fig. 9(b).

d) Spring constant (K_s): The assistive force is used when *fatigue* is *M* and *H*, and is reduced to zero otherwise (see Table V). Hence, we have defined three fuzzy variables, *low* (*L*), *medium* (*M*), and *high* (*H*) as shown in Figure 9(c).

e) Stop signal (stop): The stop signal is only used to stop the exercise when *fatigue* is *VH* (see Table V). As a result, we have defined only two fuzzy variables, namely, *yes* and *no*, for this linguistic variable as shown in Fig. 9(d).

IV. TEST RESULTS

This section evaluates the proposed fuzzy controller with five healthy young subjects who participated in the experiments mentioned in Section III-A. The use of a subset of subjects involved in the proposed system development does not significantly bias the evaluation of the proposed system because the experiment used for the development of the intelligent system employs pre-defined force patterns whereas

the experiment used in this evaluation employs varying force patterns. The experiment uses the same linear target positions and time constraint (5 sec) to reach a target as described in Section III-A. The target positions are repeated until the intelligent system stops the exercise. At the beginning of each exercise, the participant was instructed to use maximum speed and to follow the optimal path to reach a target position. The participants were allowed to go slowly within the given time limit. The system assists users in case of slow speed in order to motivate them; however, it stops the exercise if a user is not motivated and goes beyond a very slow speed limit. For this experiment, T_{max}=5 and e_{max}=6 are used (see Eq. 1). FIS-2 initially assumes zero fatigue for fatigue estimation. The exercise is stopped if the *Stop* output of the fuzzy inference system is greater than 0.8.

The rest of this section briefly describes the experimental results. Figs. 10 and 11 summarize all the experimental results and show the best-fit curves of fatigue estimation and output control signals for each experiment. The *target index* in the figures refers to the index of the current target used in the exercise. Note that the intelligent system repeats the same target positions as described in Fig. 4 with increasing target number until the exercise stops.

The speed and error values do not change monotonically, instead, the signals include peaks and valleys, which also imply increase and decrease in fatigue values. Each subject follows a different strategy and produces a different exercise duration. For example, the subject corresponding to the green color starts with a very high speed and low error; however, he/she fails to continue this performance resulting in high fatigue around the 30th target. As a result, the fuzzy controller uses negative values of ΔF_r, low values of K_d, and high values of K_s (see Fig. 11) to assist and motivate the user to continue the exercise. The subject continues the exercise with the assistance of the controller and reaches the maximum fatigue around the 275th target when the system stops the exercise. The results of the other subjects can be similarly described. Overall, the subject representing the blue color uses relatively lower average speed, lower error, and higher exercise duration than those of the previous subject. Whereas the subject representing the black color uses relatively high speed, similar error level, and higher exercise duration compared to the previous subject. The experimental results, in general, show that the proposed fuzzy controller produces appropriate control signals to motivate the user to extend the exercise duration; however, as a whole, the exercise is extended according to intention and ability of each subject which produces different exercise duration.

Table VI shows exercise durations, average fatigue and force parameter values to reach a target in the experiments. The results are sorted according to exercise duration of the experiments. It is evident from the data that the average fatigue to reach a target is very close to each other in the experiments, however, this is achieved with different combinations of F_r, K_d, and K_s. Hence, our proposed fuzzy system is successful in producing similar average fatigue values in the experiments and is able to produce different control signals to extend the exercise duration for each case.

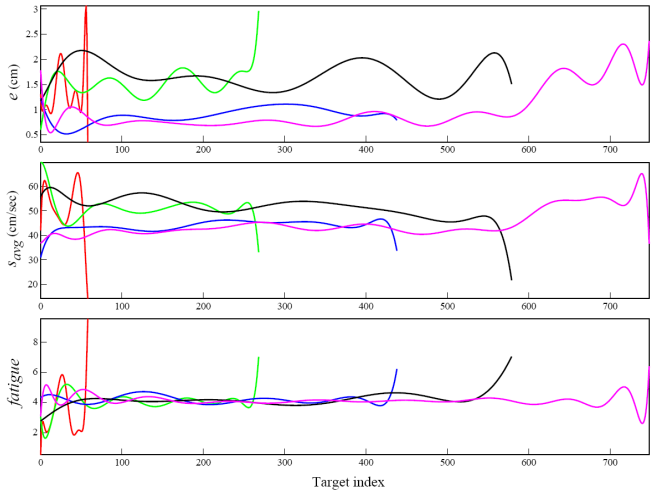

Fig. 10. Summary of fatigue estimation

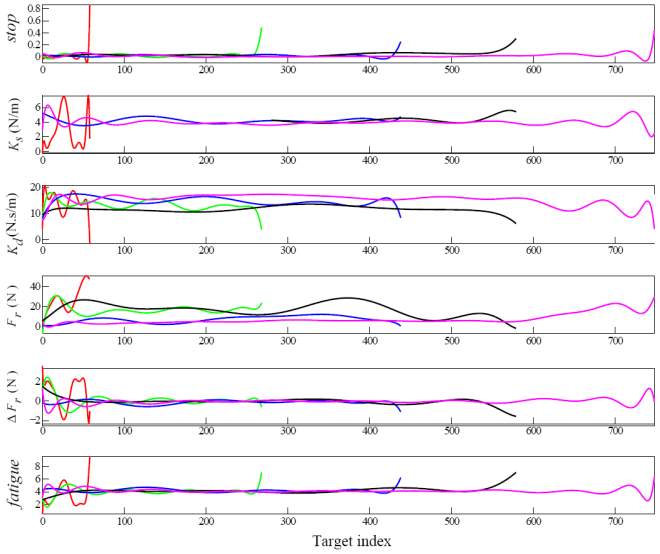

Fig. 11. Summary of output control signals

TABLE VI
SUMMARY OF THE RESULTS

Exercise Duration (sec)	Average output values to reach a target			
	fatigue	F_r (N)	K_d $\left(\frac{\text{N.s}}{\text{m}}\right)$	K_s $\left(\frac{\text{N}}{\text{m}}\right)$
49.49	3.41	27.15	14.40	2.83
198.16	4.0400	16.7200	13.2900	4.0600
330.51	4.2100	7.2100	14.7600	4.2200
492.99	4.2100	16.8200	11.6800	4.3200
561.15	4.1300	7.2300	15.3800	3.9900

V. LIMITATIONS AND FUTURE WORK

The major drawbacks observed in the proposed system are as follows: 1) it lacks the learning capability to update ranges of the MFs of the fuzzy inference system, 2) it only investigates linearly placed target positions, 3) it does not incorporate motion compensations, e.g. shoulder-hike, trunk rotation and lean-forward, for decision-making, 4) finally, it

has only been tested with healthy subjects for automating the rehabilitation exercise. Muscle fatigue of healthy persons, however, may significantly differ from that of post-stroke survivors [19, 20, 21]. As a result, the FISs need to be tuned to fit the stroke survivors.

Hence, our future work will address these issues and include pilot testing with stroke survivors.

VI. CONCLUSION

This paper describes the development of an intelligent system for autonomous guidance of post-stroke reaching exercise using a haptic robotic device. The main goal of the decision-making system is to estimate the unobservable fatigue state of the patient using the observable performance of the reaching exercise and to take appropriate actions so that the patient can extend the exercise duration with better control performance. This work employs fuzzy logic to implement the intelligent system since the performance analysis and fatigue estimation is governed by subjective assessment and often can be generalized by a set of rules. This work conducts a set of experiments to deduce a general set of rules that estimate fatigue in terms of observed speed and error during the exercise. The rules also exploit the capability of the haptic device in order to create artificial resistive and assistive forces according to the fatigue state of the patient. The fuzzy inference system is formed using the proposed rules to automate the reaching exercise. The preliminary test results show that the proposed intelligent system can successfully apply a combination of resistive and assistive forces in order to gauge user fatigue and thus extend the exercise duration using variable resistance levels. We are currently in the process of recruiting stroke survivors to conduct trials with the developed system.

ACKNOWLEDGMENT

The authors gratefully acknowledge Quanser Inc. for their technical support.

REFERENCES

[1] Heart and Stroke Foundation of Canada: Stroke Statistics [http://www.heartandstroke.com/site/c.ikIQLcMWJtE/b.3483991/k.34A8/Statistics.htm#stroke]

[2] American Heart Association: Stroke Statistics [http://www.americanheart.org/presenter.jhtml?identifier=4725]

[3] S. E. Fasoli, H. I. Krebs, and N. Hogan, "Robotic technology and stroke rehabilitation: Translating research into practice," *Topics in Stroke Rehabilitation*, vol. 11, no. 4, pp. 11-19, 2004.

[4] L. R. Caplan, Stroke, New York: Demos Medical Publishing, 2006.

[5] A. Gupta and M. K. O'Malley, "Design of a haptic arm exoskeleton for training and rehabilitation," *IEEE/ASME Trans. Mechatronics*, vol. 11, no. 3, pp. 280–289, June 2006.

[6] D. J. Reinkensmeyer, L. E. Kahn, M. Averbuch, A. McKenna-Cole, B. D. Schmit, and W. Z. Rymer, "Understanding and treating arm movement impairment after chronic brain injury," *Progress with the ARM guide, Journal of Rehabilitation Research and Development*, vol. 37, no. 6, pp. 653-662, 2000.

[7] P. S. Lum, C. G. Burgar, P. C. Shor, M. Majmundar, and M. Van der Loos, "Robot-assisted movement training compared with conventional therapy techniques for the rehabilitation of upper-limb motor function after stroke," *Archives of Physical Medicine and Rehabilitation*, vol. 83, no. 7, pp. 952-959, 2002.

[8] F. Amirabdollahian, R. Loureiro, E. Gradwell, C. Collin, W. Harwin, and G. Johnson, "Multivariate analysis of the Fugl-Meyer outcome measures assessing the effectiveness of GENTLE/S robot-mediated stroke therapy," *Journal of NeuroEngineering and Rehabilitation*, vol. 4, no. 4, pp. 1-16, 2007.

[9] H. I. Krebs, N. Hogan, M. L. Aisen, and B. T. Volpe, "Robot-aided neurorehabilitation," *IEEE Transactions on Rehabilitation Engineering*, vol. 6, no. 1, pp. 75-87, 1998.

[10] J. Yoon, B. Novandy, C-H Yoon, K-J Park, "A 6-DOF Gait Rehabilitation Robot With Upper and Lower Limb Connections That Allows Walking Velocity Updates on Various Terrains," *IEEE/ASME Trans. Mechatronics*, vol. 15, no. 2, pp. 201 – 215, April 2010.

[11] Q. Qiu, D. A. Ramirez, S. Saleh, G. G. Fluet, H. D. Parikh, D. Kelly, and S. Adamovich, "The New Jersey Institute of Technology - Robot-Assisted Virtual Rehabilitation(NJIT-RAVR) system for children with cerebral palsy: A feasibility study," Journal of Nueroengineering and Rehabilitation, vol. 6, no. 40, 2009.

[12] E. Vergaro, M. Casadio1, V. Squeri, P. Giannoni, P. Morasso, and V. Sanguineti, "Self-adaptive robot training of stroke survivors for continuous tracking movements," *Journal of NeuroEngineering and Rehabilitation*, vol. 7, no. 13. 2010.

[13] M. S. Ju, C. C. K. Lin, D. H. Lin, I. S. Hwang, and S. M. Chen, "A rehabilitation robot with force-position hybrid fuzzy controller: Hybrid fuzzy control of rehabilitation robot," IEEE Transactions on Neural Systems and Rehabilitation Engineering, vol. 13, no. 3, pp. 349-358, 2005.

[14] D. Erol, V. Mallapragada, N. Sarkar, G. Uswatte, and E. Taub, "Autonomously adapting robotic assistance for rehabilitation therapy," Paper presented at the First IEEE/RAS-EMBS International Conference on Biomedical Robotics and Biomechatronics, Pisa, Italy , 20-22 February 2006.

[15] L. Marchal-Crespo and D. J. Reinkensmeyer, "Review of Control Strategies for Robotic Movement Training after Neurologic Injury," Journal of Neuroengineering and Neurorehabilitation, vol. 6, no. 20, 2009.

[16] J. V. Basmajian and C. J. De Luca, *Muscles Alive* (5th edition), Baltimore, MD: Williams and Wilkins, 1985.

[17] T. J. Ross, *Fuzzy Logic with Engineering Applications* (3rd edition). Chichester, West Sussex, U.K. : Wiley, 2010.

[18] P. Kan, J. Hoey and A. Mihailidis, "Automated upper extremity rehabilitation for stroke patients using a partially observable Markov decision process," *AAAI Fall Symposium on AI in Eldercare,* 2008.

[19] A. M. Horstman, K. H. Gerrits, M. J. Beltman, P. A. Koppe, T. W. Janssen, and A. de Haan, "Intrinsic Properties of the Knee Extensor Muscles After Subacute Stroke," *Archives of physical medicine and rehabilitation*, vol. 91, no. 1, pp. 123-128, 2010.

[20] E. D. Toffola, D. Sparpaglione, A. Pistorio, M. Buonocore, "Myoelectric manifestations of muscle changes in stroke patients," *Archives of physical medicine and rehabilitation*, vol. 82, pp. 661–665, 2001.

[21] R. Dattola, P. Girlanda, G. Vita, M. Santoro, M. L. Roberto, A. Toscano, et al. "Muscle rearrangement in patients with hemiparesis after stroke: an electrophysiological and morphological study," *Eur Neurol,*. vol. 33: pp. 109–114, 1993.

[22] M. Barnes, B. Dobkin, and J. Bogousslavsky, Recovery after stroke, United Kingdom: Cambridge University Press, 2005.

[23] P. Lam, D. Hebert, J. Boger, H. Lacheray, D. Gardner, J. Apkarian, and A. Mihailidis, "A haptic-robotic platform for upper-limb reaching stroke therapy: Preliminary design and evaluation results," *Journal of NeuroEngineering and Rehabilitation*, vol. 5, no. 15, doi: 10.1186/1743-0003-5-15, 2008.

[24] L. Sherwood and R. Kell, *Human Physiology: from Cells to Systems* (1st edition). Toronto, ON: Nelson Education Ltd, pp. 282-283, 2010.

[25] Benjamin Y. Tseng, Sandra A. Billinger, Byron J. Gajewski, and Patricia M. Kluding, "Exertion Fatigue and Chronic Fatigue Are Two Distinct Constructs in People Post-Stroke," *Stroke (Journal of American Heart Association)*, doi: 10.1161/STROKEAHA.110.596064, 2010.